Journal of Thermal Analysis and Calorimetry (2018) 133:1099–1107
https://doi.org/10.1007/s10973-018-7116-z

Chemical kinetics and thermodynamics of the AlN crystalline phase formation on sapphire substrate in ammonia MBE

D. S. Milakhin[1] · T. V. Malin[1] · V. G. Mansurov[1] · Y. G. Galitsyn[1] · K. S. Zhuravlev[1,2]

Received: 14 September 2017 / Accepted: 24 February 2018 / Published online: 5 March 2018
© Akadémiai Kiadó, Budapest, Hungary 2018

Abstract

Chemical kinetics of a two-dimensional (2D) AlN layer formation on the (0001) sapphire (Al_2O_3) surface during nitridation as function of ammonia flux and temperature is investigated by reflection high-energy electron diffraction. The process on the surface is described in framework of a chemical reactions kinetic model including interaction between partially reduced aluminum oxide species (AlO) and chemisorbed NH_2 particles for the temperature range < 1210 K. The experimentally determined AlN formation rates as functions of both the temperature and the ammonia pressure are successfully described by a simple set of kinetic equations. Calculated maximum rate of the process well agrees with the experimental values. It was found that AlN formation rate is independent from temperature for the temperature range > 1210 K. In this range, the process is described as a phase transition in frame of lattice gas model. Precision measurement of 2D AlN lattice parameters during the nitridation process detects the value of 0.301 nm. This value strongly differs from bulk value of wurtzite AlN structure 0.311 nm, but it coincides exactly with a characteristic structure parameter of the oxygen-deficient (0001) Al_2O_3 surface with reconstruction $(\sqrt{31}\times\sqrt{31})R \pm 9°$. We assume that this coincidence is the result of minimizing the elastic stresses at the heterojunction of the 2D AlN and the (0001) Al_2O_3 layer.

Keywords Reflection high-energy electron diffraction (RHEED) · Surface processes · Molecular beam epitaxy · III-nitrides · Nitridation

Introduction

III-nitrides are direct-gap semiconductors with an energy band gap of 0.7 eV (InN) and 3.4 (GaN) to 6.2 eV (AlN) [1, 2]. These materials and their solid alloys are actively used in the creation of light-emitting diodes, laser diodes, UV photodetectors [3–5]. The III-N heterostructures with a two-dimensional electron gas are actively used to create powerful microwave and power transistors [6–8].

To date, III-nitrides are successfully grown on foreign substrates (sapphire, Si) despite the huge lattice mismatch (13–15% for sapphire, $\sim$ 20% for Si). Special substrate surface treatment (nitridation) and thin AlN film as a buffer layer are frequently used on sapphire or silicon substrate to improve crystal quality of subsequent epitaxial III-nitrides layers in both molecular beam epitaxy (MBE) and MOCVD growth. However, there is still no agreement according to the mechanisms of AlN epitaxy initiation. For example, Uchida et al. [2] showed that an exposition of the Al_2O_3 substrate under active nitrogen flux at elevated temperatures and subsequent growth forms crystal–amorphous–crystal sequence of layers with an AlN_xO_{1-x} amorphous layer. On the other hand, it was found that the AlN/Al_2O_3 interface is crystalline and abrupt with epitaxial relationship: (0001)AlN ∥ (0001)Al_2O_3 and [11–20] AlN ∥ [1–100]Al_2O_3 [4]. Grandjean et al. found [9] that during nitridation the lattice parameter of crystalline AlN epitaxial layer drastically changes from Al_2O_3 bulk value 0.275 nm to AlN bulk value 0.311 nm. On the other hand, Wang et al. using in situ grazing incidence real-time X-ray diffraction show that the initial and final strains for AlN during nitridation are similar and they are around 1.5% relative to the bulk AlN value [10]. Besides, there is

✉ D. S. Milakhin
dmilakhin@isp.nsc.ru

1 Rzhanov Institute of Semiconductor Physics, Siberian Branch of the Russian Academy of Science, pr. Lavrentieva 13, Novosibirsk, Russia 630090

2 Novosibirsk State University, Novosibirsk, Russia 630090

inconsistency for the effect of temperature on the nitridation rate: according to experimental data of Ref. [4] the rate decreases with increasing temperature, but in [11] it was shown that the nitridation rate is independent of temperature. Hence, more information about initial stage of AlN formation is still needed to improve the understanding of the process.

Recently ultrathin two-dimensional (2D) layers of III-nitrides (GaN, AlN, InN) attract a lot of interest as a possible candidate for experimental fabrication of new graphite-like layers or graphene-like monolayer (ML) [12–16]. These layers possess a number of unusual properties comparing with the normal bulk materials as it was revealed by ab initio calculations [14, 15]. Besides, the 2D AlN graphite-like sheets are attractive as a dielectric material for nanoelectronics and also it is predicted that silicene is stable when encapsulated between two thin graphite-like AlN layers [16].

Previously a lot of experimental and theoretical efforts were undertaken to elucidate the formation of an ultrathin AlN layer during a sapphire surface nitridation before an epitaxial growth of GaN-based structures, see for example [2, 4, 11, 17, 9, 10]. But so far there is neither reasonable atomic structure model of AlN/Al_2O_3 interface nor agreement according to a mechanism of the AlN formation. Cho et al. [4] and Dwikusuma and Kuech [17] studied the formation of the nitridated layer by X-ray photoelectron spectroscopy (XPS) and concluded that temporal evolution of AlN thickness could be fit by a $\sqrt{D\tau}$ growth law (where D denotes diffusion coefficient of nitrogen and τ denotes the time), which suggests a diffusion-limited growth. While XPS gives a signal proportional to the near-surface chemical concentrations, it is difficult to make a clear calibration between the signal level and effective film thickness. Moreover, usual XPS (non-angle resolved) is insensitive to the crystallographic state of the chemical species in question and usually operates in a mode in which the nitridation process is stopped for measurement (i.e., ex situ). The kinetic measurements are reported relatively sparse. In the paper [11] the sapphire nitridation process was modeled as “counterdiffusion of anions (N^{3-} and O^{2-}) in the rigid cation (Al^{3+}) framework.” But it makes no sense because the free N^{3-} particle does not really exist. Then, according to the proposed model the nitridated layer thickness for the same exposition time should be proportional to ammonia pressure ($\sim$ P), but presented experimental data show that the thickness is almost independent of pressure. Additionally, the reflection high-energy electron diffraction (RHEED) data presented in the paper [17] show the 3D AlN islands formation (transmission spots are visible), but authors have used the 2D planar model of the nitridation layer.

Wang et al. [10] presented more detailed kinetics measurements of the sapphire nitridation by a grazing incidence diffraction technique. It was shown that the detailed early-stage growth evolution could not be fitted by a simple square root function. The authors proposed to use a formal kinetic model of Johnson–Mehl–Avrami–Kolmogorov (JMAK) that was further developed to describe the AlN layer nucleation and growth isothermal kinetics [10]. This approach has demonstrated better fitting of calculated kinetic curves to the experimental dependences [18]. The authors have concluded that the AlN growth being controlled by thermally activated processes such as diffusion and chemical reactions [10]. However, simple estimations of the AlN maximum growth rate from the presented experimental kinetic curves at temperatures of 470 and 1020 K give the values of 0.41 and 0.16 ML min^{-1}, respectively. Another manner of estimation demonstrates that the nitridated layer thickness of 0.6 nm is reached after 38 min at 470 K and during 62 min at 1020 K. These simple estimations seem to be at odds with the conclusion above. Moreover, the JMAK model does not elucidate the mechanism of AlN formation from the precursors: active nitrogen gas and sapphire. We believe that the nitridation mechanism could be better described in the framework of realistic surface reaction kinetics for the precursors in the spirit of Zhdanov’s approach [19].

In the present work, the early stages of the AlN crystal formation on the (0001) Al_2O_3 surface during nitridation in ammonia molecular beam epitaxy (MBE) have been investigated by the reflection high-energy electron diffraction (RHEED) technique as a function of NH_3 pressure and substrate temperature. A kinetic scheme of surface reactions is developed, and thermodynamic aspects of the process are discussed.

Experimental

The sapphire surface nitridation was studied in molecular beam epitaxy equipment (MBE-32P, Riber) with an ammonia gas source. An initial surface of sapphire used for nitridation is clean and smooth (RMS $\sim$ 0.2 nm) as it was found by atomic force microscopy (AFM) measurement over the 5 $\times$ 5 μm^2 area. The basic pressure in the growth chamber was 1.33 $\times$ 10^{-7} Pa. The back side of the (0001) Al_2O_3 substrate was covered by 450-nm-thick Mo film to provide the radiative heating of the sapphire from a high-temperature oven. Before the experiments, the substrate was annealed at 1070 K for 2 h. The growth temperature on the surface of sapphire substrate was measured by pyrometer. The pyrometer data were calibrated by fitting of the substrate thermal radiation spectra by the Planck’s law, and the procedure is described in details elsewhere [20].

For the experiments on kinetics of nitridation, the ammonia flux was varied in range of 10–400 $cm^3 min^{-1}$ at temperature of 1150 K, and the substrate temperature was varied in range of 1120–1320 K at the ammonia flux of 25 $cm^3 min^{-1}$.

RHEED is a unique in situ method in the studying of surface structure, surface reconstructions phase transitions and chemical reactions kinetics on the surface. The reconstructions phase transitions are characterized by the behavior of the long-range-order parameter. The long-range-order parameter (η) can change discontinuously (the first-order phase transition) or continuously (the second-order phase transition) [21]. In general, an intensity (I) of the diffraction beam associated with the crystalline phase under consideration is directly determined by the long-range-order parameter $I = \eta^2$ [22]. The time dependency of the intensity of the diffraction beam makes it possible to study the kinetics of chemical reactions if crystalline phases are involved. At the same time, the diffraction experiment requires the use of complex techniques: obtaining of ultrahigh vacuum, use of molecular beams, the preparation of atomically clean and smooth surfaces of crystals, as well as the diffraction equipment itself being complicate.

Evolution of the total RHEED pattern during the ammonia treatment of the sapphire surface is monitored by a CCD-based system, and the intensity of sapphire and AlN spots was measured. Small area sample (4 mm in diameter) was used to decrease the influence of a temperature and ammonia flux inhomogeneity and also to decrease the effect of sapphire surface charging by the primary electron beam of RHEED (Fig. 1a, b).

Experimental results and discussion

Kinetics of nitridation

A typical RHEED pattern of the initial sapphire surface is shown in Fig. 2a (T = 1150 K). There is no reconstruction on the surface. Diffraction pattern after the nitridation process at the same temperature (τ = 500 s, F_{NH3-} = 25 $cm^3 min^{-1}$) is shown in Fig. 2b. Appearance of a new diffraction streak is clearly seen, and at the same time the sapphire diffraction spots were weakened.

Evolutions of the intensities of (02) Al_2O_3 and (01) AlN streaks as a function of nitridation time at T = 1150 K demonstrate opposite characters as it is shown in Fig. 3; the first intensity decreases and the last one increases. After few minutes of the NH_3 exposure, a saturation of the AlN intensity was observed.

Curves of the (01) AlN intensity as function of time, measured at different substrate temperatures, are shown in Fig. 4. Each of the curves was normalized by the own saturation intensity value. The saturation of AlN spot intensity is also clearly visible for the high temperature curves in Fig. 4. The behavior of the intensities manifests a conversion of the Al_2O_3 initial surface layer into crystalline AlN. Then, the normalized curve could be interpreted as an extent of the Al_2O_3 surface layer transformation into AlN as the function of time. Let us denote the extent of the transformation as α ($0 \leq \alpha \leq 1$). From the kinetic curves, the maximum of the rate $(d\alpha/d\tau)_{max}$ (in units of s^{-1}) was determined for each temperature and the dependence is shown in Fig. 5.

Two regions with different behaviors of the rate of AlN formation were found: there is strong temperature dependence at comparatively low temperatures (T < 1210 K), and the rate is almost constant at higher-temperature region (T > 1210 K).

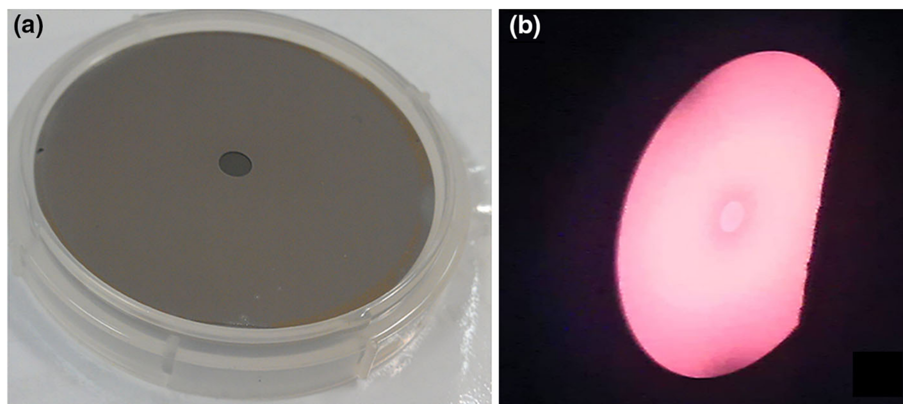

Fig. 1 Photographs of the small area sample: **a** at room temperature and **b** sample in growth chamber of MBE-32P machine at T = 1170 K

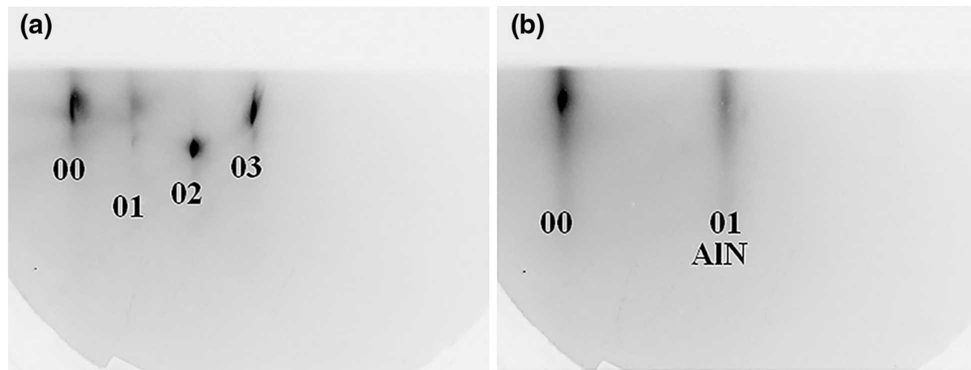

Fig. 2 **a** Diffraction pattern of a clean (0001) Al_2O_3 near the symmetric azimuth [11–20] and **b** diffraction pattern of the same surface after the nitridation process

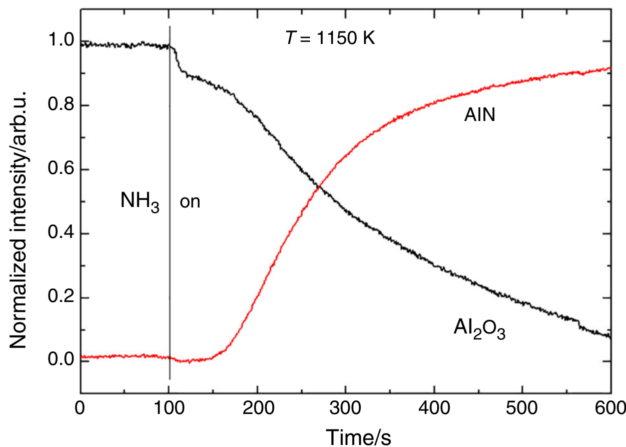

Fig. 3 Intensity behavior for the diffraction spots of sapphire and AlN

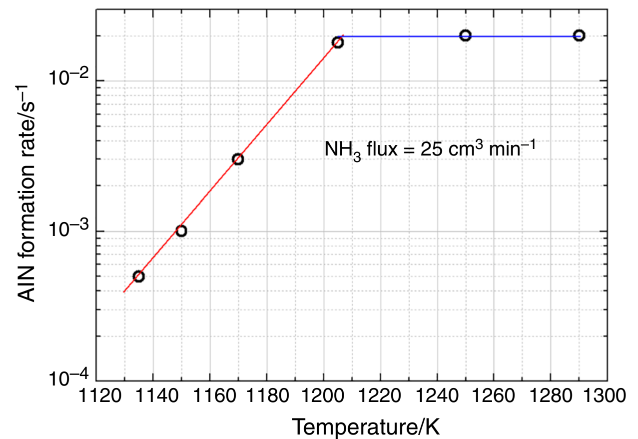

Fig. 5 Temperature dependence of maximum of the transformation rate

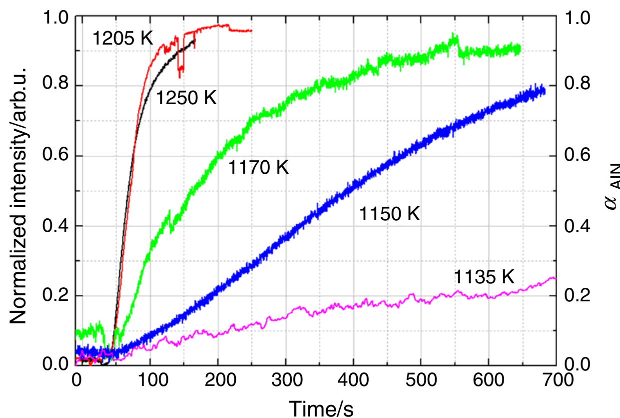

Fig. 4 Evolution of AlN intensity at different temperatures

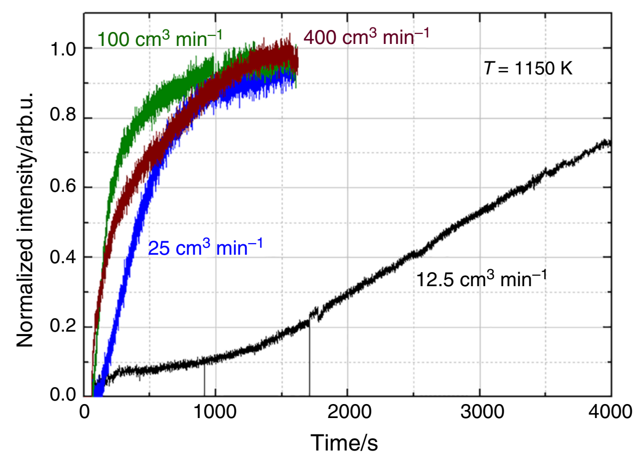

Fig. 6 AlN formation at the different ammonia fluxes: experimental kinetic curves

Kinetic curves measured at the different ammonia fluxes are shown in Fig. 6. Evidently, the rate of nitridation increases with the increase in the ammonia flux. Note that the kinetic curve has S-like shape as it is clearly seen in Figs. 4 and 6. This shape disagrees with the root square law proposed in papers [4, 17], but it is similar to data presented by Wang et al. [10]. The maximal AlN formation rate $(d\alpha/d\tau)_{max}$ as a function of the ammonia flux is shown in Fig. 7 (see experimental dots). The dependence of the

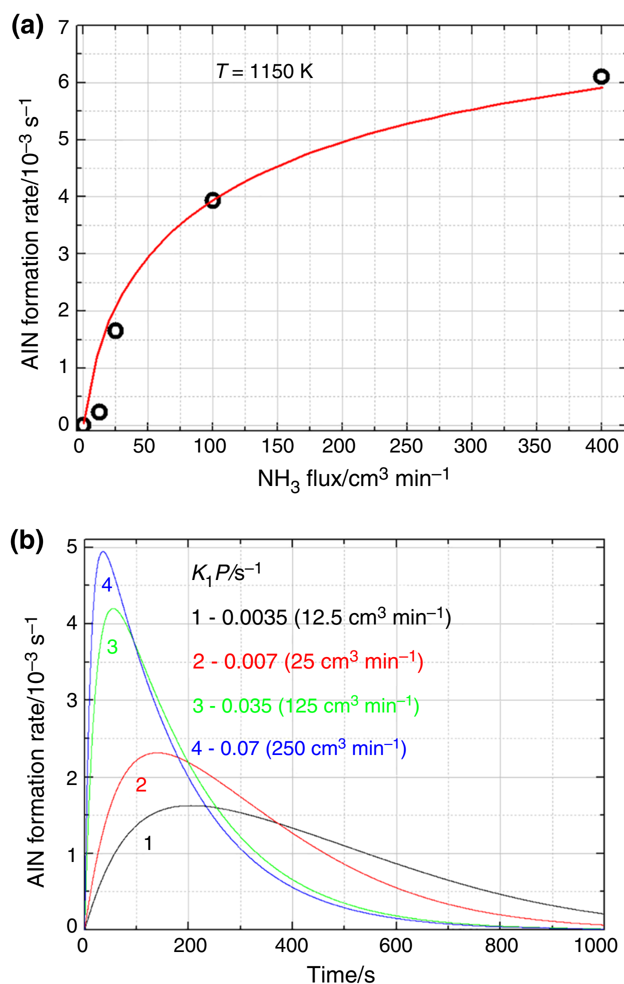

Fig. 7 **a** Maximum AlN formation rate as a function of ammonia flux: open dots—experimental data, solid line—curve calculated from a kinetic scheme developed in this work (see below) and **b** AlN formation rate calculated from a kinetic scheme (see below)

rate on pressure clearly demonstrates sublinear behavior, and it can be very roughly fitted by the square root law.

Lattice constant behavior

We have taken precision measurements of 2D AlN lattice constant evolution during the nitridation (Fig. 8).

The bulk value of 0.311 nm of the wurtzite AlN lattice constant with space group C_{6v}^4-$P6_3mc$ is well known. In contrast, the initial value of 0.301 nm for the 2D AlN layer was found in our measurements. It is important to underline that this value of 0.301 nm has fundamental meaning also for the clean (0001) Al_2O_3 surface. This characteristic value has been observed by AFM, and it has enabled to explain the commensurate superstructure $(\sqrt{31} \times \sqrt{31})R \pm 9^\circ$ of the Al_2O_3 surface [23]. A coincidence of the 2D AlN lattice parameter observed here with the characteristic structure parameter of the reconstructed

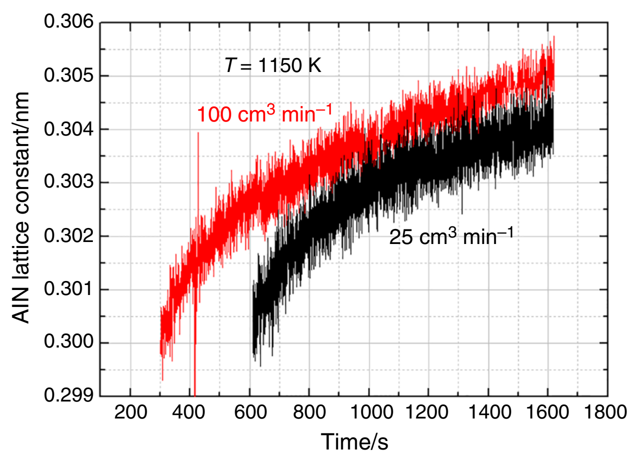

Fig. 8 AlN lattice constant evolution at the different NH_3 fluxes. The AlN signal appears earlier at the higher flux

Al_2O_3 surface can be attributed to the properties of the 2D AlN layer. Recently, it was shown that the 2D AlN lattice parameter differs from the bulk value because of formation of graphene-like hexagonal crystal structure where atoms are threefold coordinated with an sp^2-like bonding [13–15, 24]. The variability of AlN lattice constant may result from the buckling effect of the AlN nanolayers [13]. This property of the 2D AlN layer allows growing epitaxial layers of III-nitrides with reduced elastic stresses. We believe that the increase of the 2D AlN lattice parameter in Fig. 8 may results from relaxation of the AlN lattice toward the bulk value. On the other hand, one can suppose that at very beginning of nitridation crystal phase of AlNO appears with the lattice constant 0.301 nm.

Surface reactions kinetics: temperature range < 1210 K

Obviously, the AlN product formation from Al_2O_3 and NH_3 reactants is a result of successive chemical reactions on the surface. Each step of the transformation of Al_2O_3 to AlN requires overcoming some energy barrier that is the reason of the strong temperature dependence observed in the experiment in temperature range < 1210 K.

At least the following set of reactions should be taken into account. First, the aluminum cations, Al^{3+}, in the topmost Al_2O_3 surface layer are partially reduced to the Al^{2+} oxidation state (i.e., AlO formation) because of oxygen desorption during the preliminary annealing of the substrates and along with the nitridation process itself.

$$Al_2O_3 \rightarrow 2AlO + \frac{1}{2}O_2 \qquad (1)$$

This partial reduction reaction of the aluminum surface cations has been proposed by French and Somordjai to explain the formation of the sapphire surface

reconstruction [25]. Moreover, it was supposed later that the total Al_2O_3 surface decomposition occurs resulting in formation of an Al metallic state on the reconstructed surface [23, 26].

The adsorption of ammonia molecules onto the sapphire surface evidently takes place, and it happens most likely in the form of dissociative chemisorptions

$$NH_3^{gas} \xrightarrow{k_1} NH_2^{ads} + \frac{1}{2}H_2^{gas} \uparrow \quad (2)$$

This process was often observed on different surfaces of solids, see, for example, [27, 28]. Next, let us suppose that the reaction of the AlN formation occurs in the following form:

$$NH_2^{ads} + AlO \xrightarrow{k_2} AlN + H_2O \quad (3)$$

Also, the decomposition of ammonia on the surface should be taking into account:

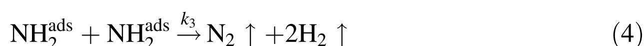

$$NH_2^{ads} + NH_2^{ads} \xrightarrow{k_3} N_2 \uparrow + 2H_2 \uparrow \quad (4)$$

Finally, the overall reaction is:

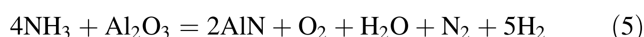

$$4NH_3 + Al_2O_3 = 2AlN + O_2 + H_2O + N_2 + 5H_2 \quad (5)$$

In Table 1, the standard thermodynamic parameters (Gibbs free energy, entropy and enthalpy) of reagents and products of chemical reaction from Eq. (5) at standard conditions (10^5 Pa, 298 K) are presented. If we subtract the reactants Gibbs free energy from reaction products Gibbs free energy multiplied by the corresponding coefficients, we obtain $\Delta G > 0$ (under standard conditions, the process is thermodynamically forbidden), and the equilibrium state ($\Delta G = 0$) comes at a temperature of 2140 K, that is rather higher than experimental temperature range. However, under the high-temperature annealing of the sapphire surface, aluminum is partially reduced to $Al^{2+}O$ (Eq. 1) with desorption of oxygen atoms (O) up to the 2 ML Al formation [23, 26]. In this case, $\Delta G < 0$, and the reaction is thermodynamically allowed.

In frame of the mean field approximation the following kinetics equations for the surface concentrations of $[NH_2]$, [AlO], [AlN] could be written:

$$\frac{d[NH_2]}{d\tau} = k_1 \cdot P \cdot (1 - [NH_2]) - k_2 \cdot [NH_2] \cdot [AlO] - k_3 \cdot [NH_2]^2 \quad (6)$$

$$\frac{d[AlO]}{d\tau} = -k_2 \cdot [NH_2] \cdot [AlO] \quad (7)$$

$$\frac{d[AlN]}{d\tau} = k_2 \cdot [NH_2] \cdot [AlO] \quad (8)$$

where P is ammonia pressure.

The numerical solution of these equations gives a good agreement with the experimental data (Fig. 9) in the temperature range $T < 1210$ K if the kinetics constants k_i take the following values:

$$k_1 P = 6 \times 10^4 \cdot \exp(-144.73\,\text{kJ mol}^{-1}/kT)\,[s^{-1}] \quad (9)$$

$$k_2 = 7 \times 10^{19} \cdot \exp(-511.37\,\text{kJ mol}^{-1}/kT)\,[s^{-1}] \quad (10)$$

$$k_3 = 3 \times 10^{13} \cdot \exp(-385.94\,\text{kJ mol}^{-1}/kT)\,[s^{-1}] \quad (11)$$

It should be noted that the constants are not corresponding to elementary chemical reactions on the surface, because each of the proposed reactions (6)–(8) represents a complicate process.

The developed reaction kinetics is also confirmed by the experimental data of AlN formation rate as a function of ammonia pressure. Using the same values of the kinetic constants, we calculated the dependence of the maximal AlN formation rate as a function of the ammonia pressure P. The dependence is shown in Fig. 7a (solid line). A good agreement of the calculated curve with the experimental values is clearly seen. Several examples of the calculated AlN formation rate as a function of time are shown in Fig. 7b at different pressures.

Table 1 Standard thermodynamic values under normal conditions

Formula	ΔH/kJ mol^{-1}	ΔS/J mol^{-1} K^{-1}	ΔG/kJ mol^{-1}
Al_2O_3 (s alpha corundum)	− 1675.274	50.919	− 1581.971
NH_3 (g)	− 46.108	192.339	− 16.485
AlN (s)	− 317.984	20.167	− 287.023
O_2 (g)	0	205.029	0
H_2 (g)	0	130.587	0
H_2O (g)	− 241.819	188.715	− 228.589
N_2 (g)	0	191.502	0
AlO (g)	83.680	218.279	57.739
Al (s)	0	28.326	0

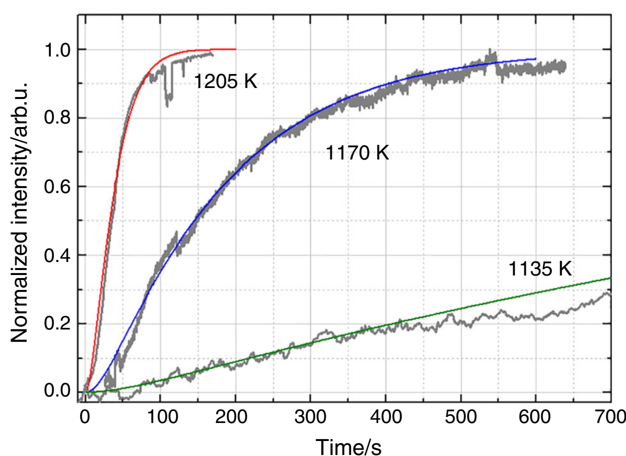

Fig. 9 The broken curves are the experimental kinetic curves, and smooth curves were calculated from the presented kinetic scheme by numerical fitting

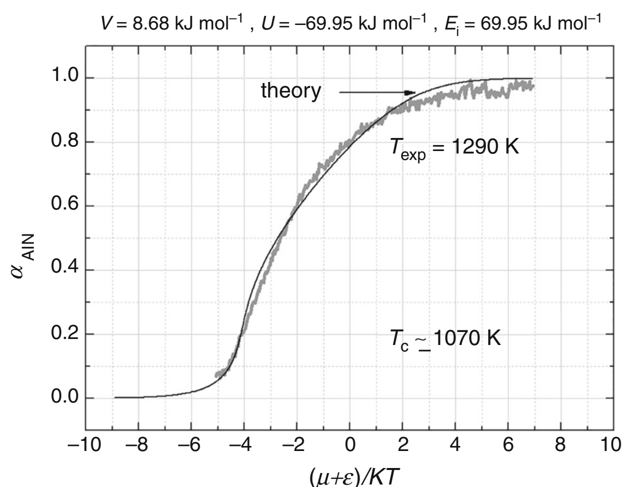

Fig. 10 Comparison of the calculated three-parameter isotherm and the experimental curve (broken)

Surface phase transition: high temperature range

In the high-temperature region ($T > 1210$ K), as it is shown in Fig. 5, the rate of AlN formation does not depend on the temperature; hence, in this case the chemical reactions do not limit the formation process. In this case, the AlN crystalline phase formation can be limited by a surface phase transition in AlN lattice gas [29].

The lattice gas model [29, 30] seems to be very helpful to describe the AlN phase formation. Obviously, at the very beginning stage of the nitridation the separate AlN-like small particles (or AlN lattice gas) appear on the sapphire surface and their concentration increases with nitridation time. Phase transition in the lattice gas to a condensed phase definitely occurs if there is a lateral interaction between the AlN filled cells.

A surface phase transition can be described by the one-parameter Fowler–Guggenheim isotherm [23], or by a more universal three-parameter isotherm [29]. The experimental isotherm is asymmetric, but the one-parameter isotherm is always symmetric. Therefore, it is necessary to use the three-parameter isotherm:

$$\frac{\mu+\varepsilon}{kT} = \ln\left[\frac{\alpha}{1-\alpha}\right] + \left[\frac{E_{\mathrm{i}}\alpha}{kT} - \frac{U/kT}{1+\exp[(V-U\alpha)/kT]}\right] \tag{12}$$

where μ is AlN chemical potential; α is a coverage of the surface by the AlN filled cells (or the extent of reaction introduced above); ε is a vertical interaction energy of AlN cells with substrate; U, V, E_{i} are parameters of lateral interaction between neighbor AlN cells; and k is Boltzmann constant.

Equation (12) should be considered as the implicit function of α from the argument $(\mu + \varepsilon)$/kT. Variation of the argument in range from -5 to $+5$ is sufficient to change α from 0 to 1. The value of $(\mu + \varepsilon)$/kT increases with nitridation time because of the increase in entropy part of the chemical potential as the AlN cells are accumulated on the surface.

Good agreement (see Fig. 10) of the calculated isotherm with experimental curve at $T_{\mathrm{exp}} = 1290$ K is found by numerical fitting for the following parameters of lateral interaction: $E_{\mathrm{i}} = 69.95$ kJ mol^{-1} is the pairwise lateral repulsive energy between neighboring filled AlN cells, $U = -69.95$ kJ mol^{-1} is a stabilization energy (energy gain with filled cell formation), and $V = 8.68$ kJ mol^{-1} is an energy loss for the formation of intermediate lattice gas cell. Usually, the symmetric isotherm has the E_{i} parameter value two times more than U [29], but in our case, we have asymmetric isotherm, so these parameters can take close or even identical values. The critical temperature of $T_{\mathrm{c}} = 1070$ K is determined by the parameters of lateral interaction. The experimental temperatures are higher than T_{c}; hence, the observed phase transition is the continuous phase transition, i.e., there is no interphase boundary between the lattice gas and condensed phase.

Conclusions

Temperature dependence of nitridation rate (AlN formation rate) is investigated, and a complicated character of the process is revealed. Two different temperature dependences of the AlN formation rate are found: strong temperature dependence at $T < 1210$ K, but the rate is not depending on temperature at range $T > 1210$ K. The kinetic scheme of the surface reactions AlN formation is developed. The values of kinetic constants for the surface

processes are determined. Good agreement of theoretical kinetics curves with experimental curves was obtained at $k_1P = 6 \times 10^4 \exp(-144.73\ \mathrm{kJ\ mol^{-1}/kT})\ [\mathrm{s^{-1}}]$, $k_2 = 7 \times 10^{19} \exp(-511.37\ \mathrm{kJ\ mol^{-1}/kT})\ [\mathrm{s^{-1}}]$ and $k_3 = 3 \times 10^{13} \exp(-385.94\ \mathrm{kJ\ mol^{-1}/kT})\ [\mathrm{s^{-1}}]$. The developed reaction kinetics is also confirmed by the experimental data of AlN formation rate as a function of ammonia pressure.

For the high temperature range, the AlN formation process is described as surface phase transition in AlN lattice gas. Parameters of lateral interaction between filled AlN cells and the critical temperature of the phase transition are determined ($T_c = 1070$ K).

Precision measurement of 2D AlN lattice parameters during the nitridation process detects the value of 0.301 nm. This value is strongly differ from bulk value of wurtzite AlN structure 0.311 nm, but it coincides exactly with a characteristic structure parameter of the oxygen-deficient (0001)Al_2O_3 surface with reconstruction $(\sqrt{31}\times\sqrt{31})R \pm 9°$. We assume this coincidence results from flexibility of the 2D AlN monolayer which provides minimization of elastic stresses at the AlN/(0001)Al_2O_3 interface.

Acknowledgements This work was supported by the Russian Foundation for Basic Research (Grant Nos. 17-02-00947, 16-02-00018, 16-02-00175).

References

1. Strite S, Morkoc H. GaN, AlN and InN: a review. J Vac Sci Technol B. 1992;10:1237.
2. Uchida K, Watanabe A, Yano F, Kouguchi M, Tanaka T, Minagawa S. Nitridation process of sapphire substrate surface and its effect on the growth of GaN. J Appl Phys. 1996;79:3487.
3. Nakamura S, Mukai T, Senoh M. Highly P-typed Mg-doped GaN films grown with GaN buffer layers. Jpn J Appl Phys. 1991;30:1708.
4. Cho Y, Kim Y, Weber ER, Ruvimov S, Liliental-Weber Z. Chemical and structural transformation of sapphire (Al_2O_3) surface by plasma source nitridation. J Appl Phys. 1999;85(11):7909.
5. Saito Y, Akiyama T, Nakamura K, Ito T. Ab initio-based approach to elemental nitridation process of α-Al_2O_3. J Cryst Growth. 2013;362:29–32.
6. Alekseev AN, Krasovitsky DM, Petrov SI, Chaly VP. Molecular-beam epitaxial growth of GaN layer with low dislocation density. Semiconductors. 2012;46:11.
7. Ing-Song Yu, Chang C-P, Yang C-P, Lin C-T, Ma Y-R, Chen C-C. Characterization and density control of GaN nanodots on Si (111) by droplet epitaxy using plasma-assisted molecular beam epitaxy. Nanoscale Res Lett. 2014;9(1):682.
8. Chen S-H, Chou P-C, Cheng S. Channel temperature measurement in hermetic packaged GaN HEMTs power switch using fast static and transient thermal methods. J Therm Anal Calorim. 2017;129:1159–68.
9. Grandjean N, Massies J, Leroux M. Nitridation of sapphire. Effect on the optical properties of GaN epitaxial overlayers. Appl Phys Lett. 1996;69(14):2017.
10. Wang Y, Özcan AS, Özaydin G, Ludwig KF, Bhattacharyya A, Moustakas TD, Zhou H, Headrick RL, Siddons DP. Real-time synchrotron X-ray studies of low- and high-temperature nitridation of c-plain sapphire. Phys Rev B. 2006;74:235304.
11. Im I, Chang J, Oh D, Park J, Yao T. Dynamic investigations of (0001) Al_2O_3 surfaces treated with a nitrogen plasma. J Ceram Process Res. 2012;13(6):783.
12. Costales A, Blanco MA, Francisco E, Solano CJF, Pendas AM. Theoretical simulation of AlN nanocrystals. J Phys Chem C. 2008;112:6667.
13. Solano CJF, Costales A, Francisco E, Pendas AM, Blanco MA, Lau K, He H, Pandey R. Buckling in wurtzite-like AlN nanostructures and crystals: why nano can be different. Comput Model Eng Sci. 2008;24(2):143.
14. Şahin H, Cahangirov S, Topsakal M, Bekaroglu E, Akturk E, Senger RT, Ciraci S. Monolayer honeycomb structures of group-IV elements and III–V binary compounds: first-principles calculations. Phys Rev B. 2009;80:155453.
15. Ivanovskii AL. Graphene-based and graphene-like materials. Russ Chem Rev. 2012;81(7):571.
16. Houssa M, Pourtois G, Afanas'ev VV, Stesmans A. Can silicon behave like graphene? A first-principles study. Appl Phys Lett. 2010;97:112106.
17. Dwikusuma F, Kuech TF. X-ray photoelectron spectroscopic study on sapphire nitridation for GaN growth by hydride vapor phase epitaxy: nitridation mechanism. J Appl Phys. 2003;94:5656.
18. Das A, Goswami M, Krishnan M. Crystallization kinetics of Li_2O–Al_2O_3–GeO_2–P_2O_5 glass–ceramics system. J Therm Anal Calorim. 2017;131:2421–31.
19. Zhdanov VP. Elementary physicochemical processes on solid surfaces. New York: Plenum; 1991.
20. Malin TV, Mansurov VG, Gilinskii AM, Protasov DY, Kozhukhov AS, Vasilenko AP, Zhuravlev KS. Growth of AlGaN/GaN heterostructures with a two-dimensional electron gas on AlN/Al_2O_3 substrates. Optoelectron Instrum Data Process. 2013;49(5):429 **(in Russia: Avtometriya. 2013;49(5):17)**.
21. Zangwill A. Physics at surfaces. Cambridge University Press, Cambridge. 1988;5:111.
22. Wang GC, Lu TM. Physical realization of two-dimensional Ising critical phenomena: oxygen chemisorbed on the W(112) surface. Phys Rev B. 1985;31:5919.
23. Lauritsen JV, Jensen MCR, Venkataramani K, Hinnemann B, Helveg S, Clausen BS, Besenbacher F. Atomic-scale structure and stability of the $\sqrt{31} \times \sqrt{31}R\pm 9°$ surface of Al_2O_3 (0001). Phys Rev Lett. 2009;103:076103.
24. Tsipas P, Kassavetis S, Tsoutsou D, Xenogiannopoulou E, Golias E, Giamini SA, Grazianetti C, Chiappe D, Molle A, Fanciulli M, Dimoulas A. Evidence for graphite-like hexagonal AlN nanosheets epitaxially grown on single crystal Ag(111). Appl Phys Lett. 2013;103:251605.
25. French TM, Somorjai GA. Composition and surface structure of the (0001) face of alpha-alumina by low-energy electron diffraction. J Phys Chem. 1970;74:2489.
26. Vilfan I, Lancon F, Villain J. Rotational reconstruction of sapphire (0001). Surf Sci. 1997;392:62.
27. Fattal E, Radeke M, Reynolds G, Carter EA. Ab initio structure and energetics for the molecular and dissociative adsorption of NH_3 on Si(100)-2 × 1. J Phys Chem B. 1997;101:8658.
28. Pignedoli CA, Di Felice R, Bertoni CM. Dissociative chemisorption of NH_3 molecules on GaN(0001) surfaces. Phys Rev B. 2001;64:11330.

29. Galitsyn YuG, Lyamkina AA, Moshchenko SP, Shamirzaev TS, Zhuravlev KS, Toropov AI. Self-assembled quantum dots: from Stranski-Krastanov to droplet epitaxy. In: Belucci S, editor. Self-assembly of nanostructures. New York: Springer; 2012. p. 127–200.
30. Yamaguchi H, Horikoshi Y. Surface structure transitions on InAs and GaAs (001) surfaces. Phys Rev B. 1995;51:9836.